Note. The Effect of a Commercial Extended Egg Albumen on the Microstructure of Icing

J. Buckman[1] and C. Viney[2,*]

[1]*Department of Petroleum Engineering;* [2]*Department of Chemistry, Heriot-Watt University, Edinburgh EH14 4AS, Scotland*

Royal icing (sugar with extended egg albumen) and glacé icing (sugar only) were examined by light microscopy and environmental scanning electron microscopy. These techniques allow a variety of structural information to be characterized without damage occurring to the specimen. Microstructures were compared in an effort to explain the enhanced hardness and toughness exhibited by Royal icing. The inclusion of extended egg albumen was found to affect both the nucleation and the growth of crystalline material in the icing. The extended egg albumen promoted spherulitic morphologies, finer-scale microstructures, multiple phases, and improved interlocking and cohesion at internal interfaces. The retention of air bubbles in Royal icing provided additional sites at which crack growth could be arrested.

Key Words: icing, environmental scanning electron microscopy, polarized light microscopy, egg albumen, microstructure, spherulite, hardness, toughness

Royal icing (merengue, azúcar con clara de huevo añadida) y *glacé icing* (sólo azúcar) se analizaron mediante microscopía de luz polarizada y microscopía electrónica de barrido. Estas técnicas permiten obtener información estructural de la muestra sin causarle ningún daño. Las microestructuras se compararon con el fin de explicar el aumento de dureza y elasticidad del *Royal icing*. La adición de la albúmina afectó a la nucleación y al crecimiento de cristales en el azúcar glaseado. La adición de clara de huevo también favoreció la formación de morfologías esferolúticas, de microestructuras más finas, de fases múltiples y mejoró el entrelazado y la cohesión entre interfases internas. La retención de burbujas de aire en el interior del *Royal icing* facilitó puntos adicionales con los que evitar la aparición de grietas.

Palabras Clave: merengue, azúcar glacé, microscopía, microestructura, albúmina de huevo, esferulitas, dureza, elasticidad

INTRODUCTION

The simplest recipe for icing ('frosting' in North America) involves preparation of a slurry of finely powdered sugar in water. This mixture is applied to the surface of a cake and allowed to dry into a decorative layer. If a small amount of powdered albumen (or fresh egg white) is added to the mixture, a significantly harder and tougher product known as Royal icing is formed on drying. Royal icing is especially favored on traditional British Christmas cakes, as well as on wedding and other festive cakes where icing has to support the weight of the higher tiers. This paper describes how a readily available commercial ingredient, consisting of extended hen egg albumen, affects the microstructure of icing. The increased hardness and toughness of the icing are accounted for in terms of the microstructural changes. Such knowledge can help to reduce the amount of trial-and-error effort when formulating recipes that achieve other desirable combinations of mechanical properties.

*To whom correspondence should be sent (e-mail: c.viney@hw.ac.uk)
Received 19 November 2001; revised 29 January 2002.

Food Sci Tech Int 2002;8(2):109–115

ISSN: 1082-0132
DOI: 10.1106/108201302024587

MATERIALS AND METHODS

Materials

Our investigation started with a typical recipe for Royal icing (Murfitt, 1994). This recipe calls for 15 mL (1 tablespoon) dried egg albumen (sieved), 90 mL (6 tablespoons) tepid water, and 450 g icing sugar (sifted) that yields almost 500 g of material. It is best

to measure all solids by weight rather than volume to facilitate re-scaling of the recipe so that smaller quantities of icing can be prepared in the laboratory, and to optimize reproducibility of the icing composition. A trial weighing of five aliquots of a commercially available albumen-based ingredient used in Royal icing (Crestawhites, Renshaw Scott, Liverpool) revealed that 15 mL equates to 8.09 g on average for this material. Also to promote reproducibility, we adopted a quantitative interpretation of ''tepid'', taking this description to mean that the water is initially at 40 °C.

Crestawhites contains approximately 55.7% dried egg white (Renshaw product technical specification no. 04034/0004), the balance being accounted for by sugar (20.0%), potato starch (14.3%), pregelatinized starch (5.6%), stabilizer E405 (2.3%) and citric acid (2.1%). Doubling the amount of Crestawhites, relative to the amount of pure albumen called for in the typical Royal icing recipe (Murfitt, 1994), therefore yields an overall albumen : sugar ratio just slightly higher than that in the recipe. Experiments were performed in July, under warm and relatively humid ambient conditions, so any increase above the standard albumen : sugar ratio will promote hardening of the Royal icing (Murfitt, 1994). To facilitate transmitted light microscopy, it was necessary to set the icing in a thin layer on a glass substrate. The standard recipe produced a slurry that was too stodgy to spread sufficiently thin, so we increased the volume of water by 50%. Thus, the compositions that we used when formulating material for microstructural characterisation were: 0.36 g Crestawhites, 3 mL water and 10 g icing sugar (Silver Spoon, Peterborough, UK) for Royal icing; and 3 mL water and 10 g icing sugar for glacé icing.

Royal icing was prepared by placing the dry Crestawhites into a clean bowl and using a clean whisk to blend in the water until the liquid was smooth, in keeping with the original recipe (Murfitt, 1994). Icing sugar was then mixed in with a wooden spoon, adding small quantities at a time, to produce a lump-free slurry that had a cream-like consistency. A similar procedure – omitting the Crestawhites – was used to produce glacé icing.

Samples for characterization by light microscopy were prepared by introducing a small amount of the mixture at one end of a glass microscope slide. A glass cover slip was placed over the slurry and then displaced rapidly along the length of the slide while simultaneously being pressed downwards. Most observations were conducted on material that solidified in the thin ''smears'' deposited behind the cover slip by this process; the very slow rate at which material under the cover slip dries is not representative of the conditions under which icing sets under practical conditions of use.

Light Microscopy

An Olympus BH-2 transmitted polarized light microscope was used to examine samples under a variety of imaging conditions (Viney, 1989, 1990):

(a) Samples were viewed between crossed polars (i.e., a polarizer and crossed analyzer) to reveal optically anisotropic microstructural features.
(b) Without changing the field of view, a first-order red (sensitive tint) plate was inserted between the sample and the analyzer. This serves a number of purposes: to enhance contrast, to allow isotropic regions of sample to be easily distinguished from isotropic background (both are in extinction between crossed polars), to provide information about the orientation distribution of optically anisotropic regions in the sample, and to facilitate exposure metering by the camera.
(c) Again without changing the field of view, both the sensitive tint plate and the analyzer were withdrawn, so that the sample could be observed in plane polarized light. This imaging mode emphasizes discontinuities in the microstructure; it therefore provides a means of discriminating between dark lines in (a) and/or (b) that are a consequence of optical anisotropy, and those that arise from the scattering of light at abrupt boundaries.

Images were recorded on Agfa film (ISO 400/27 °) and processed commercially to obtain standard 15 cm × 10 cm (6 in × 4 in) prints. To present colour micrographs for reproduction as monochrome images, prints were scanned electronically at 600 dpi, reds and yellows were desaturated, cyans and blues were saturated, and the image mode was converted to greyscale. Longer-wavelength colours (and of course white) therefore appear light in the final images, while shorter-wavelength colours (and of course black) appear dark.

Environmental Scanning Electron Microscopy

The structure of samples was also studied with a Philips LaB6 XL30 Environmental Scanning Electron Microscope (ESEM). Microscopy was performed in low-vacuum mode, in a water vapor atmosphere. Under these conditions it is possible to examine samples that are not normally vacuum compatible, and to do so without any form of additional sample preparation or the need to coat the sample with a conductive material such as gold or carbon (Cameron, 1994; Thiel et al. 1997; Donald, 1998; Fletcher et al. 1999).

Samples of icing dried onto glass microscope slides were placed on the ESEM stage. The ESEM chamber was then set to pump to a vacuum of 0.5 Torr. Once 'Pre-vac' was reached, the chamber was automatically cycled ('flooded') twice between 0.1 and 0.9 Torr. The latter allows the ingress of water vapor (from water held within a conical flask behind the ESEM), which is used to amplify the image signal, and to negate any charge build up on the surface of the sample. The chamber was

then held at a vacuum of 0.5 Torr, and microstructural characterization was performed.

Secondary electron imaging was performed with a Large Field Gaseous Secondary Electron Detector (LFGSED), at a working distance of 7.5 mm, and an operating voltage of 20 kV. Backscattered electron (BSE) images were obtained with a solid state backscattered detector, at a working distance of 10 mm and an operating voltage of 20 kV.

RESULTS AND DISCUSSION

Glacé Icing

Figures 1 and 2 respectively show light microscopy and ESEM images of glacé icing. In Figure 2, the image obtained with the secondary electron detector (top) receives a signal from all irradiated surfaces of the crystals (Newbury, 1975), allowing the darkest areas to be identified as voids. The image obtained with backscattered electrons (bottom) resolved more detail, as expected (Newbury, 1975), but its susceptibility to the effects of specimen charging was greater than that of the secondary electron image.

The microstructure is dominated by large prismatic crystals, with typical sizes in the range 50–200 μm. Crystal surfaces are flat, and they are for the most part featureless across all the magnifications accessed by the two types of microscopy. The boundaries between the crystals are easily distinguishable and there is no evidence that neighbouring crystals are in any way bonded together. Irregularly shaped voids between crystals are scattered through the microstructure; some examples are labelled (V) in Figures 1 and 2. All these microstructural features are consistent with a low resistance to both deformation and crack propagation (Kingery et al. 1976; Kelly and Macmillan, 1986; Smallman and Bishop, 1995). The poor cohesivity between crystals ensures that the bulk material is soft. Together with the absence of mechanical interlocking between adjacent crystals, the straight crack paths, and the large distances that a crack can travel before encountering a crystal that it must detour around, the poor cohesivity also ensures that the material is easy to break. Holes with sharp corners act as efficient stress concentrators, and therefore as points of failure initiation.

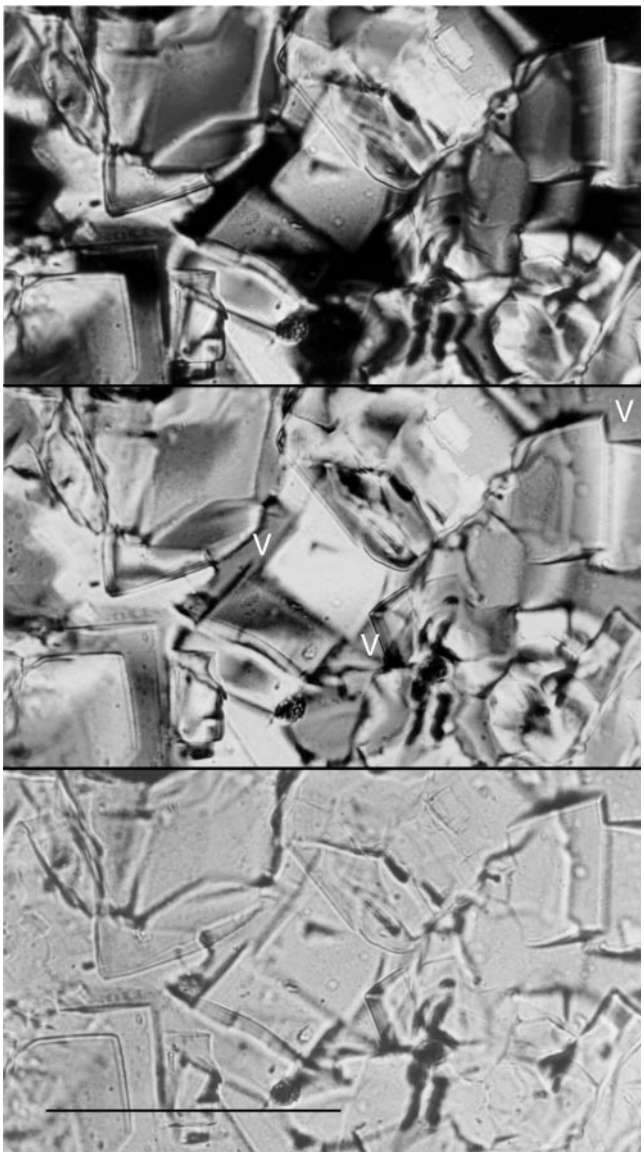

Figure 1. Polygonal microstructure of glacé icing solidified on a glass substrate and imaged by light microscopy. The scale bar represents 100 μm. Some examples of intercrystalline voids are labelled (V). Top: view between crossed polars. Middle: view between crossed polars, with sensitive tint plate inserted in 45° orientation between sample and analyzer. Bottom: view in plane polarized light (note high contrast of crystal boundaries and interfaces). The presence of a full range of greyscales in the top and middle frames demonstrates that all optical orientations are represented in the sample, i.e., there is no preferred texture.

Royal Icing

The microstructures of Royal icing differed significantly from the microstructures of glacé icing regarding the scale, morphology and number of phases present (Figures 3–6). The typical size of crystals now lies in the range 5–20 μm (Figure 3). Intergranular crack paths were more tortuous than in the glacé icing. A fine-grained microstructure translates into enhanced toughness, since the distance travelled by a crack before it must detour from its path is now reduced. Crack renucleation might be necessary after each time the growing crack is stopped at an energy-absorbing interface (Kingery et al. 1976). The crystals had an irregular

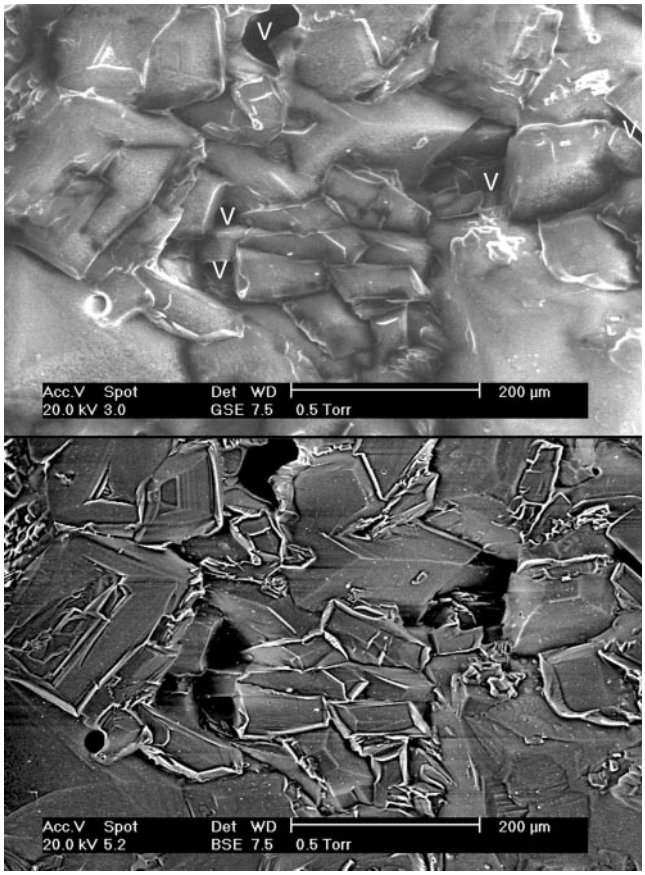

Figure 2. Glacé icing solidified on a glass substrate and imaged by ESEM. Some examples of intercrystalline voids are labelled (V). Top: secondary electron image. Bottom: backscattered electron image.

shape, which provides opportunities for mechanical interlocking. If there were voids between crystals, they were too small to be identified at this resolution. The boundaries between crystals were difficult to distinguish in plane polarized light (Figure 3, bottom); they scattered light weakly, and so did not represent abrupt discontinuities in the microstructure. This characteristic is consistent with cohesivity, hardness and toughness in a polycrystalline material (Kingery et al. 1976; Kelly and Macmillan, 1986; Smallman and Bishop, 1995).

Many regions in the Royal icing exhibited a distinctively spherulitic microstructure (Figures 4–6). A spherulitic microstructure helps to ensure an overall isotropic distribution of optically anisotropic features, so the bulk material did not exhibit net direction-dependent properties. The spherulites displayed internal fine substructure between crossed polars (Figure 4, upper left); this contrast was enhanced when the sensitive tint plate was used (Figure 4, upper right). The boundaries between spherulites were barely evident in plane polarized light; their position was only visible because they were decorated by small regions of a second precipitated phase. One example of such a

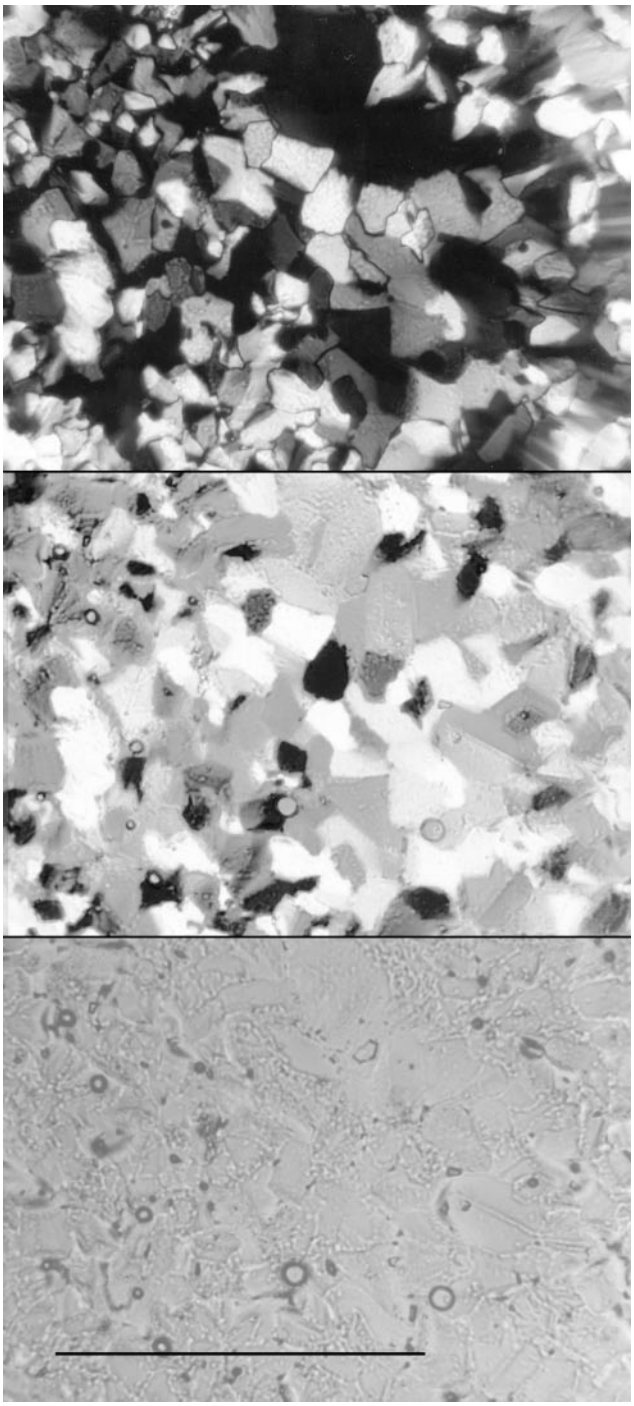

Figure 3. Polygonal microstructure of Royal icing solidified on a glass substrate and imaged by light microscopy. The scale bar represents 100 µm. Top: view between crossed polars. Middle: view between crossed polars, with sensitive tint plate inserted in 45° orientation between sample and analyzer. Bottom: view in plane polarized light (note low contrast of crystal boundaries and interfaces). The presence of a full range of greyscales in the top and middle frames demonstrates that all optical orientations are represented in the sample, i.e., there is no preferred texture.

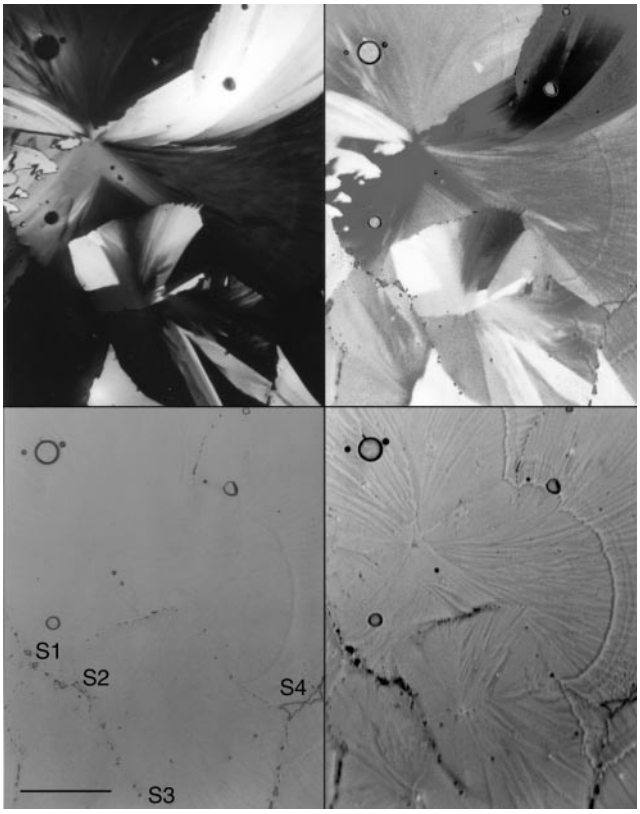

Figure 4. Spherulitic microstructure of Royal icing solidified on a glass substrate and imaged by light microscopy. The scale bar represents 100 μm. Labels S1, S2 and S3 denote the path of an interspherulitic boundary decorated by small particles of a second phase. Label S4 denotes two larger particles of the second phase. Upper left: view between crossed polars. Upper right: view between crossed polars, with sensitive tint plate inserted in 45° orientation between sample and analyzer. Lower left: view in plane polarized light (note low contrast of spherulite boundaries and internal interfaces). Lower right: slightly de-focussed view in plane polarized light (visibility of spherulite boundaries and internal interfaces is enhanced by phase contrast).

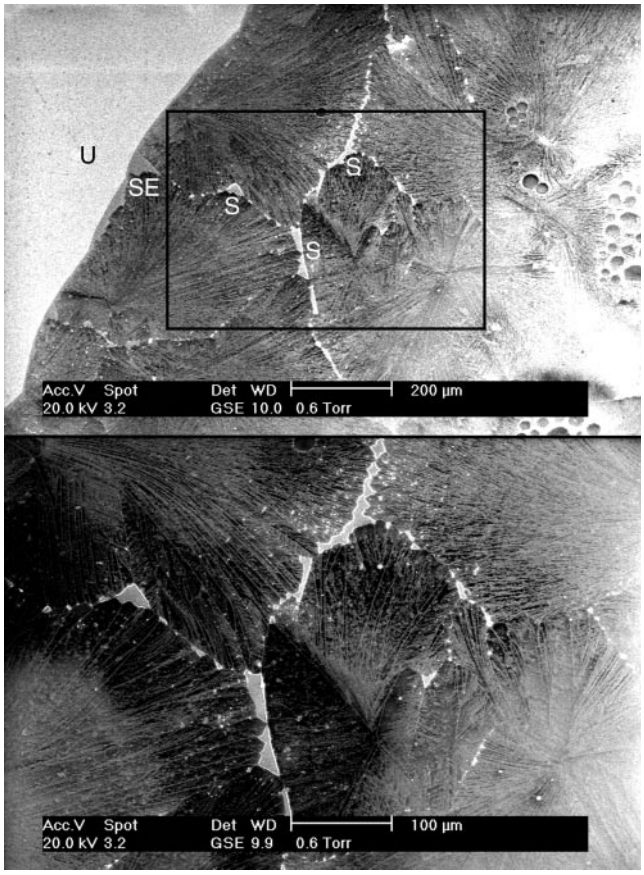

Figure 5. Royal icing solidified on a glass substrate and observed by ESEM (secondary electron images). Labels S denote interspherulitic particles of second phase, label SE denotes second phase precipitated at the edge of the sample, and label U denotes substrate on which there is no sample. The area defined by the box in the upper image is seen at greater magnification in the lower image.

boundary followed the path S1–S2–S3 labelled in Figure 4 (lower left). Two larger regions of the second phase were identified by the label S4; they lie below and to the right of this label. The fine substructure within spherulites is not visible at all in plane polarized light under standard viewing conditions, indicating a high degree of cohesivity of the internal interfaces associated with this structure. They only become apparent in a plane polarized light image if the microscope is de-focussed slightly (Figure 4, lower right), a situation that provides a rudimentary form of phase contrast (Longhurst, 1967).

The second phase observed in the interspherulitic regions by light microscopy was clearly visible when samples were imaged in the ESEM (Figure 5). The low-magnification image (Figure 5, top) demonstrates that the material designated as a second phase (labels S) was indeed material and not just empty space: the second phase is also precipitated at the edge of the sample (label SE), where it is seen in well-defined contrast relative to the empty background of the substrate (label U). The higher magnification image (Figure 5, bottom) revealed that thin layers of second phase also occured at the interfaces between the radially elongated substructures of the primary spherulitic phase. Again, the potential for the Royal icing microstructure to resist crack propagation is evident. Figure 6 displays further ESEM evidence of cohesivity in a two-phase spherulitic microstructure. In this case the microstructure also contains a high concentration of approximately spherical voids created by air bubbles trapped in the icing. We observed macroscopically that Royal icing would usually contain a mass of bubbles, while glacé icing was not sufficiently

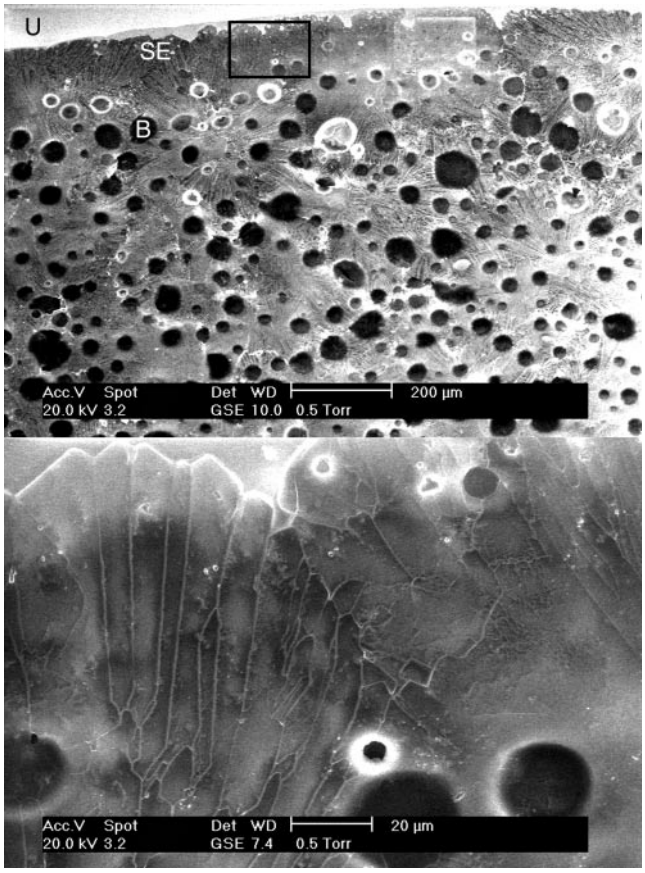

Figure 6. Royal icing solidified on a glass substrate and observed by ESEM (secondary electron images). Label SE identifies second phase precipitated at the edge of the sample, label U identifies substrate on which there is no sample, and label B identifies a spherical void created by a trapped air bubble. The area defined by the box in the upper image is seen at greater magnification in the lower image.

viscous to retain air in this way. Spherical voids differ from the irregular, stress-concentrating voids, in that they *increase* crack-stopping, ductility and fracture toughness. This effect can be demonstrated with brittle tracing paper: its fracture toughness initially increases when an increasing number of holes is punched randomly in it (Khan and Vincent, 1996).

We attempted to use the energy dispersive X-ray analysis (EDX) facility in the ESEM to investigate whether albumen was intimately dispersed through the Royal icing, or whether it was localized in particular regions such as the second phase identified in Figures 4–6. We hoped that the presence of nitrogen in the backbone of albumen protein would serve as an unambiguous marker. Unfortunately the sensitivity of the technique provides at best a 1%wt detection limit at sodium – so elements of lower atomic weight, including nitrogen, would have to be present at even greater concentration if they were to be detected. Given that the albumen was present at a concentration of 2% wt in the dry material, and that the concentration of nitrogen represents just over a third of the weight of the protein backbone alone (a smaller fraction of the protein weight if the side chains are counted too), it is unsurprising that the nitrogen content falls below the detection level of the method.

CONCLUSIONS

When a small amount of extended egg albumen (Crestawhites) is added to glacé icing to produce Royal icing, it acts as both a nucleation modifier and a growth modifier. The modification to nucleation behavior leads to a finer microstructure that contains more than one phase. The modification to growth behavior leads to grains that are less prismatic and often spherulitic.

Glacé icing contains microstructural features that facilitate deformation and crack propagation. Grains are coarse, boundaries are distinct and straight, voids are irregular, and there is little evidence of cohesion between crystals. In Royal icing, resistance to deformation and crack propagation is provided by rounded morphologies, fine microstructures, interlocking crystal boundaries, and interfacial cohesion.

Smooth spherical voids, created by trapped air bubbles in Royal icing, are poor crack nucleators but act as good crack stoppers.

The specific microstructural roles played by the several individual components in the Crestawhites are not resolved in this study, and will form the basis of further investigation.

ACKNOWLEDGMENTS

We are grateful to Amy O'Brien for careful sample preparation. Helpful information was provided by Professor Jose Miguel Aguilera (Universidad Católica de Chile), Professor A.M. Donald (University of Cambridge), and Renshaw Scott (suppliers of Crestawhites extended egg albumen). Partial funding for this work was provided by a Nuffield Science Bursary.

REFERENCES

Cameron R.E. (1994). Environmental scanning electron microscopy in polymer science. *Trends in Polymer Science* **2**: 116–120.

Donald A.M. (1998). Environmental scanning electron microscopy for the study of 'wet' systems. *Current Opinion in Colloid & Interface Science* **3**: 143–147.

Fletcher A.L., Thiel B.L. and Donald A.M. (1999). Signal components in the environmental scanning electron microscope. *Journal of Microscopy* **196**: 26–34.

Kelly A. and Macmillan N.H. (1986). *Strong Solids*. 3rd Edn. Oxford: Oxford University Press.

Khan A.A. and Vincent J.F.V. (1996). Mechanical damage induced by controlled freezing in apple and potato. *Journal of Texture Studies* **27**: 143–157.

Kingery W.D., Bowen H.K. and Uhlmann D.R. (1976). *Introduction to Ceramics*. New York: John Wiley & Sons.

Longhurst R.S. (1967). *Geometrical and Physical Optics*. London: Longmans.

Murfitt J. (1994). *Good Housekeeping Complete Book of Cake Baking and Decorating*. London: Ebury Press (Random House).

Newbury D.E. (1975). Image formation in the scanning electron microscope. In: Goldstein, J.I. and Yakowitz, H. (eds.), *Practical Scanning Electron Microscopy*. New York: Plenum Press. pp. 95–148.

Smallman R.E. and Bishop R.J. (1995). *Metals and Materials*. Oxford: Butterworth-Heinemann.

Thiel B.L., Bache I.C., Fletcher A.L., Meredith P. and Donald A.M. (1997). An improved model for gaseous amplification in the environmental SEM. *Journal of Microscopy* **187**: 143–157.

Viney C. (1989). Optical microscopy for studying molecular ordering in polymers. In: Cheremisinoff, N.P. (ed.), *Handbook of Polymer Science and Technology* Vol. 1. New York: Marcel Dekker. pp. 505–536.

Viney C. (1990). *Transmitted Polarised Light Microscopy*. Chicago: McCrone Research Institute.